

Ref. CCI #390

11/27/78
Draft

REFRIGERATION SYSTEM FOR THE ENERGY DOUBLER

CONTENTS

<u>Section</u>	<u>Title</u>	<u>Page No.</u>
I	INTRODUCTION	1
II	REFRIGERATION REQUIREMENTS	2
III	HELIUM REFRIGERATION SYSTEM	3
IV	NITROGEN REFRIGERATION SYSTEM	5
V	PERFORMANCE CHARACTERISTICS OF THE HELIUM AND NITROGEN REFRIGERATOR SYSTEMS	6
VI	PERFORMANCE CHARACTERISTICS OF THE SATELLITE REFRIGERATOR	8
VII	SYSTEM RELIABILITY	10
VIII	SYSTEM ANALYSIS	13
IX	COST OF SYSTEM OPERATION	15

REFRIGERATION SYSTEM FOR THE ENERGY DOUBLERI. Introduction

Various types of refrigeration systems have been considered for the energy doubler. The initial concept called for twelve independent refrigerators; these refrigerators would be located along the ring at every other service building. The refrigerators were rated at 1,500 W.

Before this system was implemented, it became known that surplus equipment consisting of air compressors and an air separation cold box was available. A study^[1, 2, 3] was made to determine whether this surplus equipment could be put to use as part of the energy doubler refrigeration system. As a result of this study, the present energy doubler refrigeration system evolved. A number of studies were made to determine important parameters of the system. These studies included the transport of refrigeration from the central helium liquefaction facility (CHL) to the satellite refrigerators^[4, 5], the inventory management of the helium system^[6], and the reliability of the system as a function of individual component reliability^[7, 8].

Total connected power for the system is 11.33 MW. This much power provides 19,000 W of refrigeration at 4.6°K, 1,350 liters/hr of liquid helium for lead cooling, and 54 tons/day of liquid nitrogen.

II. REFRIGERATION REQUIREMENTS

In 1973, during the early phase of the studies for the energy doubler, it was estimated that the refrigeration requirement of the doubler system would be 5 W/meter. [8]

Calculated
~~Saturated~~ heat loads of the 20 ft long dipole magnets of the doubler system are as in Table I. [2, 3]

T A B L E I

		4.4°K	80°K
Dipole	(Steady State	4.14 W	20.2 W
	(Pulsed* (AC)	13.33 W	
Quadrupole	(Steady State		
	(Pulsed	1.25 W	
B _{min} = 9 KG		B = 53 GeV/sec	
B _{max} = 42 KG			

This translates into a load of 2.86 W/meter for the dipole and ___ W/meter for the quadrupole.

In addition to the refrigeration load, electrical leads require a flow rate of cold helium vapor as follows:

The number of electrical leads to be used breaks down as follows:

III. HELIUM REFRIGERATION SYSTEM

Figures 1 and 2 show schematically the major components of the helium refrigeration system. Figure 1 shows the components located at the central helium liquefaction facility (CHL). These are:

- a) Two parallel helium compressors A and B.
- b) A single oil removal system C serving both compressors.
- c) A medium pressure helium gas storage facility D which removes or adds gas to the system upon demand.
- d) A compressor seal gas cleanup system E to repurify helium gas leaking from the compressor piston rod packings.
- e) The helium liquefier cold box F.
- f) A liquid-gaseous helium separator G in which the gas of the liquefier J-T stream is separated from the liquid and returned to the liquefier.
- g) A 5,000 gallon liquid helium storage tank H.
- h) A liquid helium pump I submerged in a liquid sump to drive liquid helium from the CHL to the distribution system of the doubler.

Figure 2 shows the major components of one of the twenty-four stations along the ring. Liquid helium circulates through the distribution line, which parallels the doubler. Excess liquid is returned to the storage dewar H of Figure 1. Each satellite station calls for liquid in an amount sufficiently

large to maintain the system of the satellite. Each service station contains a satellite refrigerator cold box M. Liquid from this cold box flows to the magnet string N through a subcooler L. At the end of each magnet string the single-phase liquid is returned as two-phase liquid. This two-phase fluid cools the magnets^[8] and is returned to the satellite refrigerator cold box M, after passing through the low pressure side of the subcooler L.

Compressors of the satellite refrigerator are located in six service buildings along the ring. Low and high pressure gas is distributed through 8 in. and 3 in. pipes, respectively. The 8 in. pipe also serves to receive the low pressure gas flow from the electrical leads and cooldown flow during the time when the doubler is cooled from ambient temperature. Helium gas is returned to the CHL after compression by the satellite refrigerator compressors through the 3 in. high pressure header.

IV. NITROGEN REFRIGERATION SYSTEM

Liquid nitrogen is required for two purposes; the central helium liquefier requires nitrogen in the liquefaction process. Also, the magnet shields are cooled by liquid nitrogen. This requirement automatically provides liquid nitrogen shielding of the liquid helium transfer line between CHL and doubler.

Figure 3 shows the schematic diagram of the nitrogen refrigeration system. Compressors, cold box, and storage tank are surplus equipment. New components are the oil removal system and turbine. A detailed description of the nitrogen reliquefaction process is given in ref. [2].

V. PERFORMANCE CHARACTERISTICS OF THE HELIUM AND NITROGEN REFRIGERATOR SYSTEMS

1. The CHL was purchased on the basis of a specification generated by Fermilab. This specification was based on the use of two parallel modified-for-helium-service air compressors with the following characteristics:

Inlet Pressure:	1.05 atm
Discharge Pressure:	12.3 atm
Flow Rate (Two Compressors):	8,573 lb/hr
Power Required (Two Compressors)	2,470 kW
Power Required (He Air Cooler)	52 kW

2. The CHL cold box was purchased under Subcontract #90641. The following performance data are part of this subcontract:

Liquid Helium Production	$\geq 4,000$ 1/hr <i>at 1.397 atm</i>
(9,900 lb/hr of He at 11.9 atm to the cold box)	at 1.397 atm
Liquid nitrogen consumption per liter of liquid He produced	$\leq .6$ <i>liter/liter</i>

3. Nitrogen Reliquefier	2,550 1/hr
Production Rate <i>based on</i>	(54 tons/day)
Based ^a Compressor Flow Rate of	37,500 lb/hr
Suction pressure	1 psig
Discharge Pressure	1,800 Psig
Power Requirement	2,540 kW

4. The nitrogen reliquefier is a closed system in which ambient temperature, low pressure (1 psig) nitrogen gas from CHL and magnet system is reliquefied. The closed system will

have gas losses. These losses will be made up through purchase of commercial liquid nitrogen. This liquid will be added to the storage tank. Refrigeration of this purchased liquid nitrogen will be used in the system. Because of this, the anticipated refrigeration capability of the liquid nitrogen refrigeration system will be augmented by 4-8 tons/day of purchased liquid nitrogen (190-390 liters/hr of liquid nitrogen).

VI. PERFORMANCE CHARACTERISTICS OF THE SATELLITE REFRIGERATOR

The satellite refrigerator may be operated in three distinctly different modes, as shown in Table II:

T A B L E I I

<u>Satellite Refrigerator Parameters</u>		
<u>Mode</u>	<u>Consumption</u>	<u>Production</u>
Satellite	92 l/hr He	690 Watt
Refrigerator	37 l/hr N ₂	445 Watt
Liquefier	60 l/hr N ₂	90 l/hr He
Nominal Compressor	$P_{in} = 1.05 \text{ atm}$ $P_{out} = 20. \text{ atm}$ $\text{Flow} = 41.1 \text{ g/sec}$	

To provide maximum refrigeration, the satellite mode is used. In order to produce 16,500 W of refrigeration at 4.5 to 4.6°K, the central helium liquefier provides 2,208 liters/hr of liquid helium. In addition, ___ liters/hr of liquid helium is supplied to cool the leads.

Power requirements of the satellite refrigerator system depend on the type of compressor employed. To date, four different types of compressors have been used. These compressors have the characteristics as shown in Table III. It should be noted that the performance of the satellite refrigerator is based on a flow rate of 41.1 g/sec through the compressor (Table II). The York compressor package was developed

T A B L E I I I

	<u>York</u>	<u>Vilter</u>	<u>Sullair</u>	<u>Mycom</u>
Type	Recip.	Recip.	Screw	Screw
Stages	3	3	1	2
Power (Connected) Bhp	200	300	400	350
Suction Pres. (Atm)	1.05	1.05	1.05	1.05
Discharge Pres. (Atm)	20.6	20.6	20	20
Throughput (g/sec)	33	37	47	49.2
Throughput (lb/hr)	262	293	373	390
Throughput as Percentage of Table II	80.5	90	114.5	120
Refrigeration @ 4.5°K	552	621	790	828

before screw compression had become acceptable for helium service. The Vilter Compressor was an alternate source of reciprocating compressor.

Both screw compressors provide excess gas flow relative to the requirement of Table II. Extra refrigeration may, therefore, be anticipated as long as the pressure drop in the low pressure gas circuit of the satellite cold box is acceptable and the wet engine can handle the larger flow rate.

Assuming the use of Mycom compressors for the satellite refrigerators, total power requirement is 8,400 bhp (6,270 kW).

VII. SYSTEM RELIABILITY

The refrigeration system consists of many separate components. All of these components have their own mean time between failures (MTBF). In order to make the system reliable, it is necessary to make the overall system as independent of individual component failures to the greatest degree. This has been accomplished in the following manner:

1. CHL Non-Operational: The satellite refrigerators will operate in a refrigerator mode without supply of liquid helium. Refrigeration capability is 600 W per satellite (no liquid helium). In order to achieve this performance, the standby warm engines need to be turned on and liquid nitrogen (45 liters/hr = 23 tons/day total) is supplied through the transfer line. Liquid helium for lead cooling may be supplied from the storage tank H (Figure 1) and compressed into gas storage by the satellite compressors for reasonable short periods of time. If the CHL is down for long periods of time, the satellite refrigerators need to be operated in a combined refrigerator-liquefier mode with reduced refrigeration output.

2. Nitrogen Refrigerator Not Operational: Liquid nitrogen will be supplied from an outside source at the rate of 2-3 trailer loads, dependent on requirement.

3. Satellite Compressor Not Operational: One compressor represents 4% of total capacity. Redistribution of gas through the 3 in. and 8 in. warm gas lines allow uniform distribution of 96% of gas flow.

4. Satellite Wet Expander Not Operational: The satellite can maintain its performance level, if 400 liters of helium per hour are added in lieu of wet expander operation. Also, the wet expander is installed as a module, which may be replaced by a complete spare unit within 2 hrs.

5. Satellite Cold Box Non-Operational: This event will shut down beam operation until the cold box is returned to service.

6. Vacuum System Non-Operational: There are a large number of vacuum systems, primarily in the liquid helium and nitrogen distribution system. The main transfer line, when constructed of twenty-five modules, may be maintained in an operating mode, when any one of the twenty-five modules is out.

Probability of the occurrence of the six listed events is impossible to determine at this time. However, occurrence of Items 2, 3, and 4 does not affect operation of the overall system.

With proper design and assembly, vacuum systems have proven to provide MTBF of 50,000 hours or more. With this MTBF, Item 6 does ^{not} affect the performance of the system. Item 5 failure most likely will be one of two types; either the insulating vacuum will fail or the cold box will plug with impurities (oil, water, or air). Again, the vacuum failure is most unlikely. Plugging of the box could be a likely event and requires that much attention is paid to system analysis for contamination of the system. Item 1 will occur fairly

frequently during the initial startup of the system, unless debugging can be accomplished prior to doubler system operation.

Type of failures most likely to occur are:

- Compressor valve and ring failures.
- Compressor cooling system failures.
- Contamination of the gas stream to the cold box with plugging of heat exchangers.

VIII. SYSTEM ANALYSIS

The system analysis concerns itself with the behavior of the total system as a function of the behavior of its elements. The analysis covers startup, steady state, and upset conditions. Typically a system is designed for steady state; the non-steady state conditions, however, are of equal importance and often require unusual features.

Following are some of the non-steady state events which the system needs to handle:

a) Magnet Cooldown:

A minimum string of magnets is approximately 400 ft long. It is coupled to a satellite refrigerator in parallel with another string of magnets. The cold weight of a complete string of twenty magnets is approximately 40,000 lb. To cool this weight, some 1.45×10^9 joules need to be removed. Liquid helium supplied by the CHL and warmed to ambient temperature will provide 1.9×10^5 joules per liter. If 200 liters per hour are available per satellite station, cooldown time per 1/24th of the ring will be of the order of 75 hours. Piping, valving and controls will be provided to carry out the cooldown of strings of magnets.

b. Magnet Quench:

The present system allows the addition of a small amount of heat into the windings of the magnets. This drives a part of the windings normal and energy deposition starts in these windings. The normal zone in the magnet grows and liquid helium

needs to be vented from the magnets at a very high rate. The helium is vented into the 8 in. low pressure header and from there through safety valves to the atmosphere. Helium gas is not vented in the tunnel. Also, the rate of venting is such that the gas cannot be compressed and stored in the gas storage facility.

c. Replacement of a Magnet:

To replace a single magnet, a string of 400 ft of magnets needs to be warmed. Time to accomplish the replacement of a magnet needs to be determined.

d) Inventory Management:

Because liquid helium is quite compressible, inventory of the operating system is difficult to determine. Some calculations [6] have been made to provide an insight into the problems associated with the accurate measurement of the inventory of the system. Figure 4 shows the uncertainty of the measurement of the loss of gas from the system. Lines 1a and 1b enclose the area of uncertainty. The figure demonstrates that a number of days are required to determine the slope of the curve and the average loss rate per day. The picture becomes considerably more difficult when operations resulting in loss of unknown quantities of gas and/or liquid are carried out.

IX. COST OF SYSTEM OPERATION

Apart from personnel, major system operational costs are the following:

- a) Power.
- b) Liquid helium.
- c) Liquid nitrogen.

The relative importance of these three items can be shown on the basis of estimated costs as follows:

Power:	\$.04 per kWh
Helium:	\$.07 per scft
Liquid Nitrogen:	\$70 per ton (\$.062 per liter)

Costs are (per day):

Power Consumption;		
11.33 x 1000 x 24 x .04	=	\$10,876.80
Helium; 7,000 x .07	=	490.00
Liquid N ₂ ; 6 x \$70	=	420.00
		<hr/>
TOTAL:		\$11,786.80

Power obviously outweighs the loss of gas by a wide margin. In order to save a sizeable amount of money, power consumption may be reduced as a function of demand for refrigeration. The system lends itself to some degree to this, as follows:

- a) One of four compressors in each cluster of satellite refrigerator compressors may be closed down to provide 75% of the maximum amount of refrigeration. This would save 1.5 MW of power or approximately 14% of the power bill.

b) Nitrogen refrigeration as provided by the modified air separation plant is not extremely efficient. This becomes evident, when comparing the cost of purchased liquid nitrogen with that manufactured on site. If the nitrogen refrigerator makes fifty-four tons per day at a cost of 2.5 MW of power, cost of liquid nitrogen per ton in terms of power alone is \$44.50. Purchased liquid nitrogen costs \$70 per ton.

c) Cost of liquid helium is not a large factor. However, at a loss rate of 7,000 scft per day some 2.5×10^6 scft of helium would be consumed per year. This number becomes significant, if and when more facilities using liquid helium go on-stream. In that case, the price of helium will go up and its cost ~~becomes~~ ^{may become} a significant factor.

It should be also pointed out that it is necessary to make a fundamental decision about the tightness of the helium system in the design stage of the system. It is very difficult, once the system has been constructed, to improve its performance.

REFERENCES

1. Energy Doubler Refrigeration System Consisting of a Central Liquefier with Satellite Stations, Etc., CCI Report No. 282-106, 2/21/75.
2. Nitrogen Reliquefier for Central Helium Liquefier, CCI Report No. 321-192, 1/7/76.
3. Fin-Fan Coolers for Helium Service, CCI Report No. 321-191, 12/12/75.
4. Transport of Refrigeration between CHL and Satellite Stations, CCI Report No. 321-202, 9/8/76.
5. Liquid Helium Transfer Line between CHL and Satellite Stations, CCI Report No. 321-209, 4/8/77.
6. Inventory Management of the Energy Doubler Helium System, CCI Report No. 321-213, 4/22/77.
7. Refrigeration System for the Energy Doubler, CCI Report No. 321-196, 4/28/76.
8. P. C. Vander Arend and W. B. Fowler: Superconducting Accelerator Magnet Cooling Systems. IEEE Transactions on Nuclear Science, Vol. NS20, No. 3, p. 119, 1973.

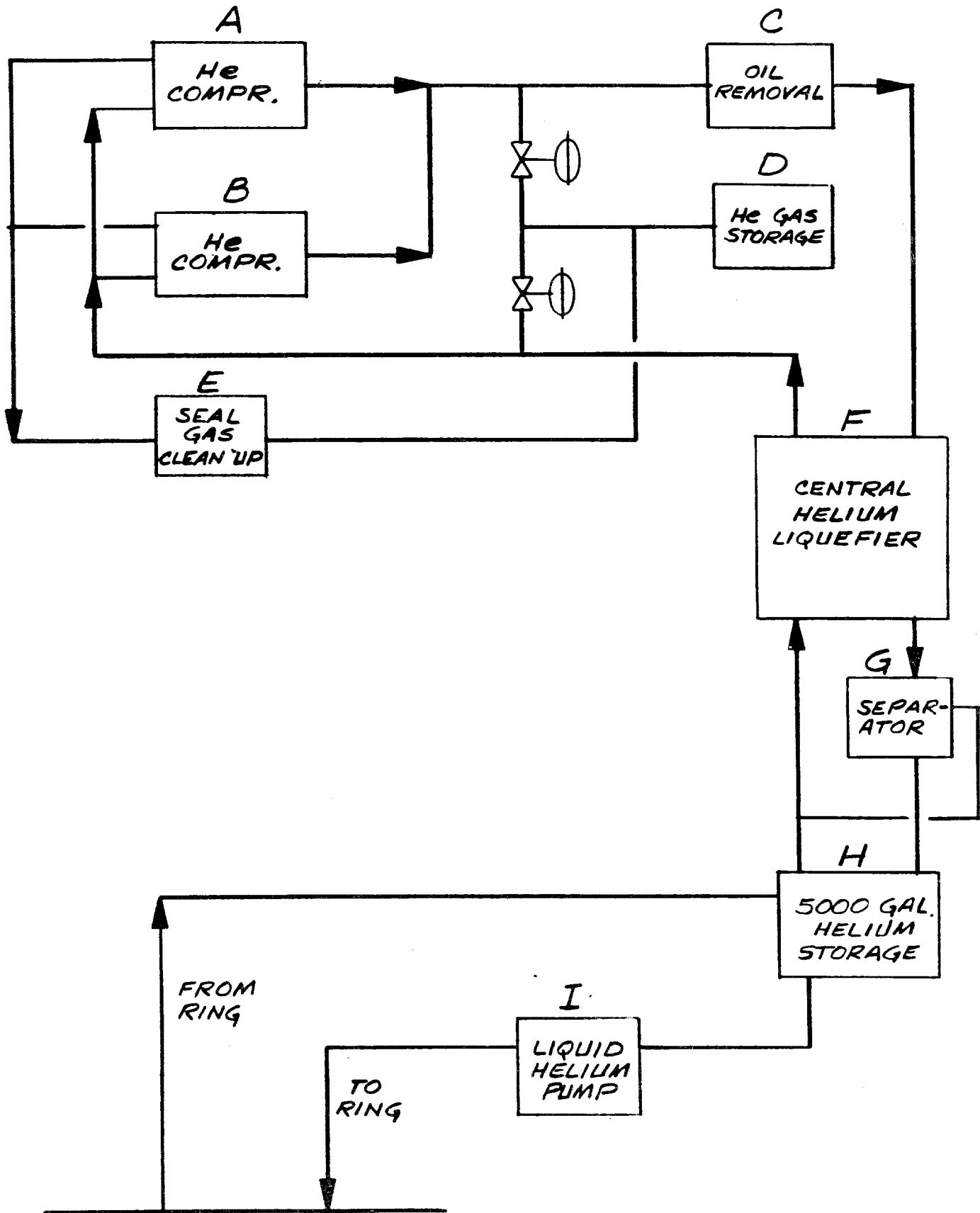


FIG. 1

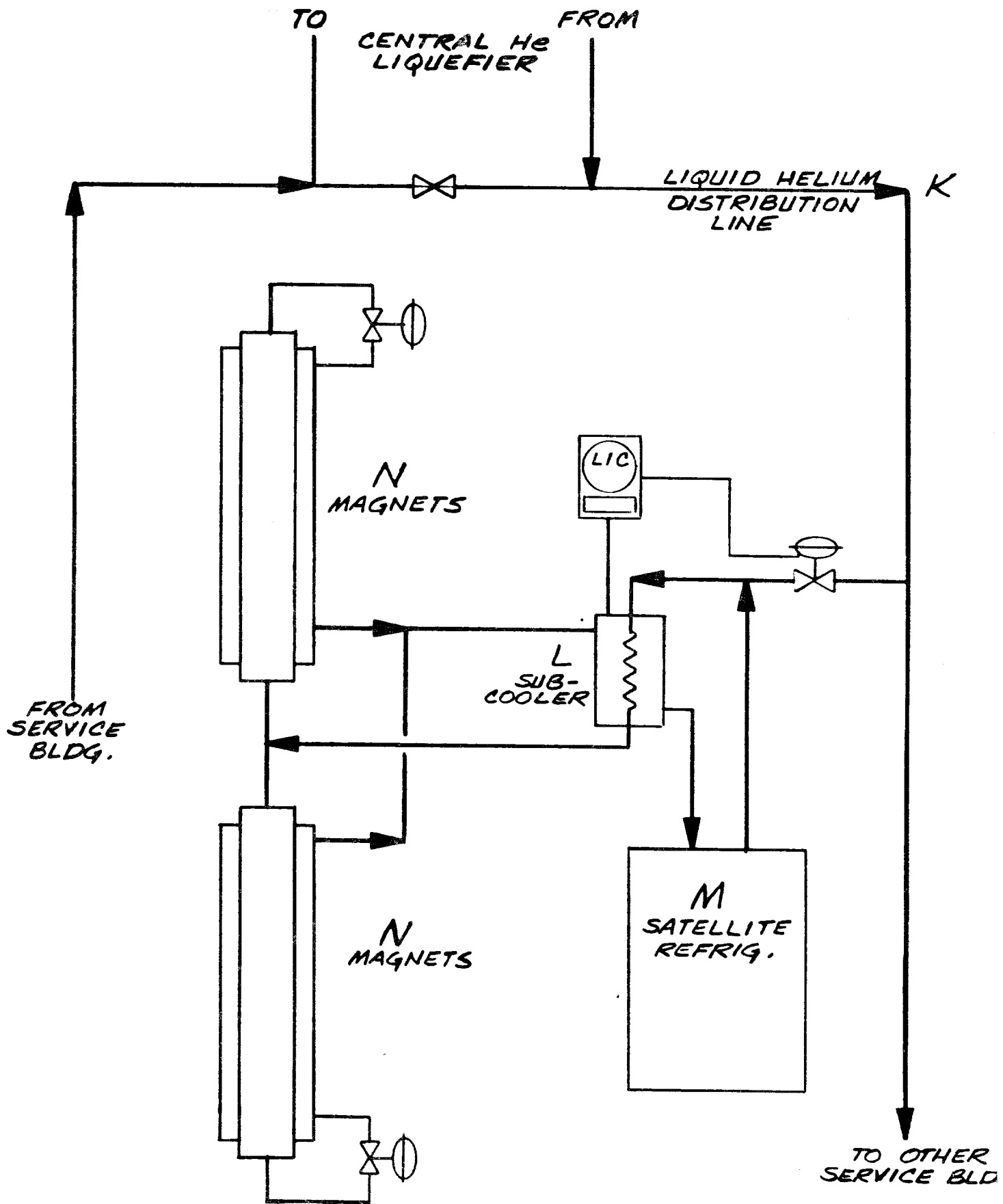


FIG - 2

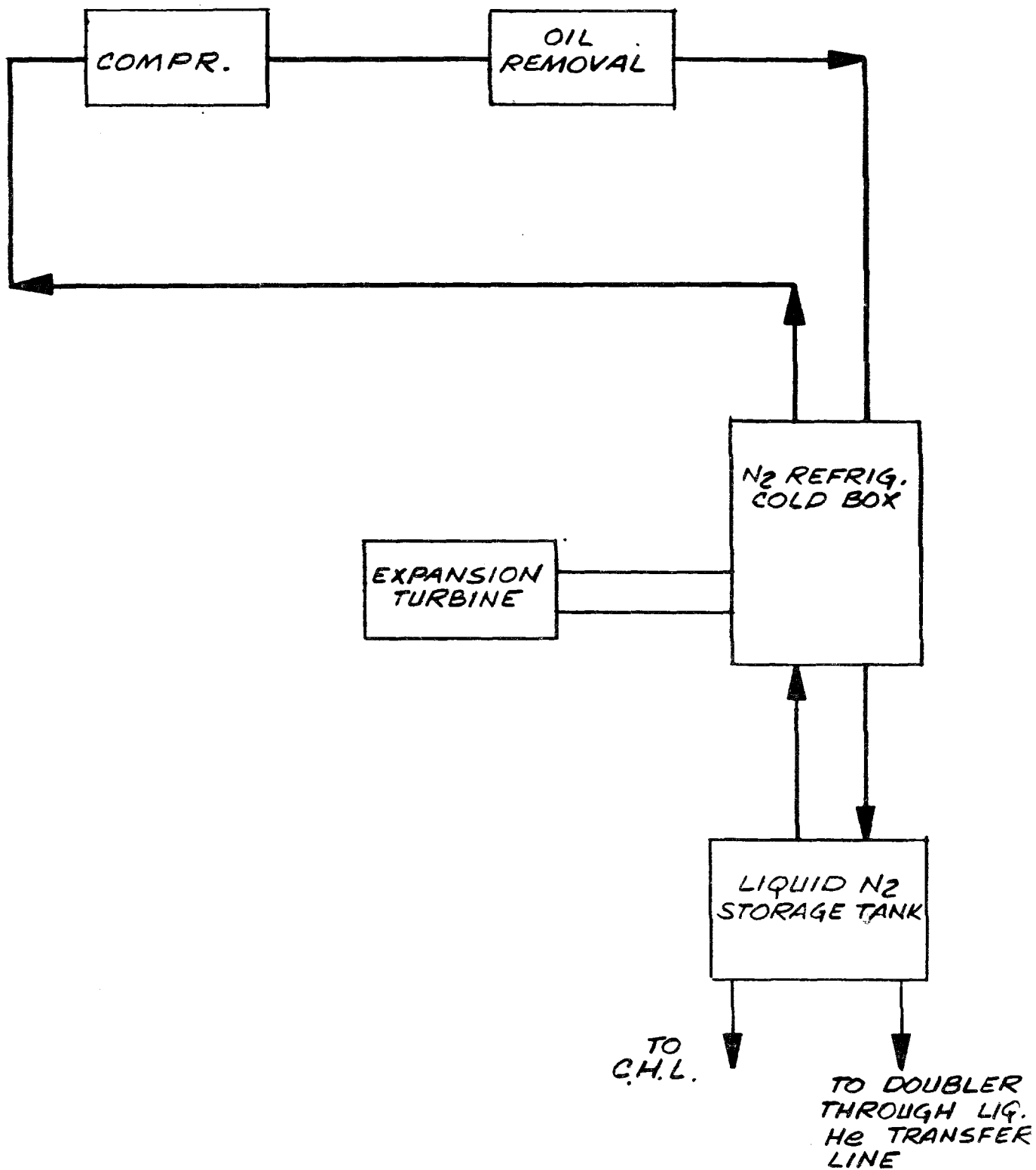


FIG - 3

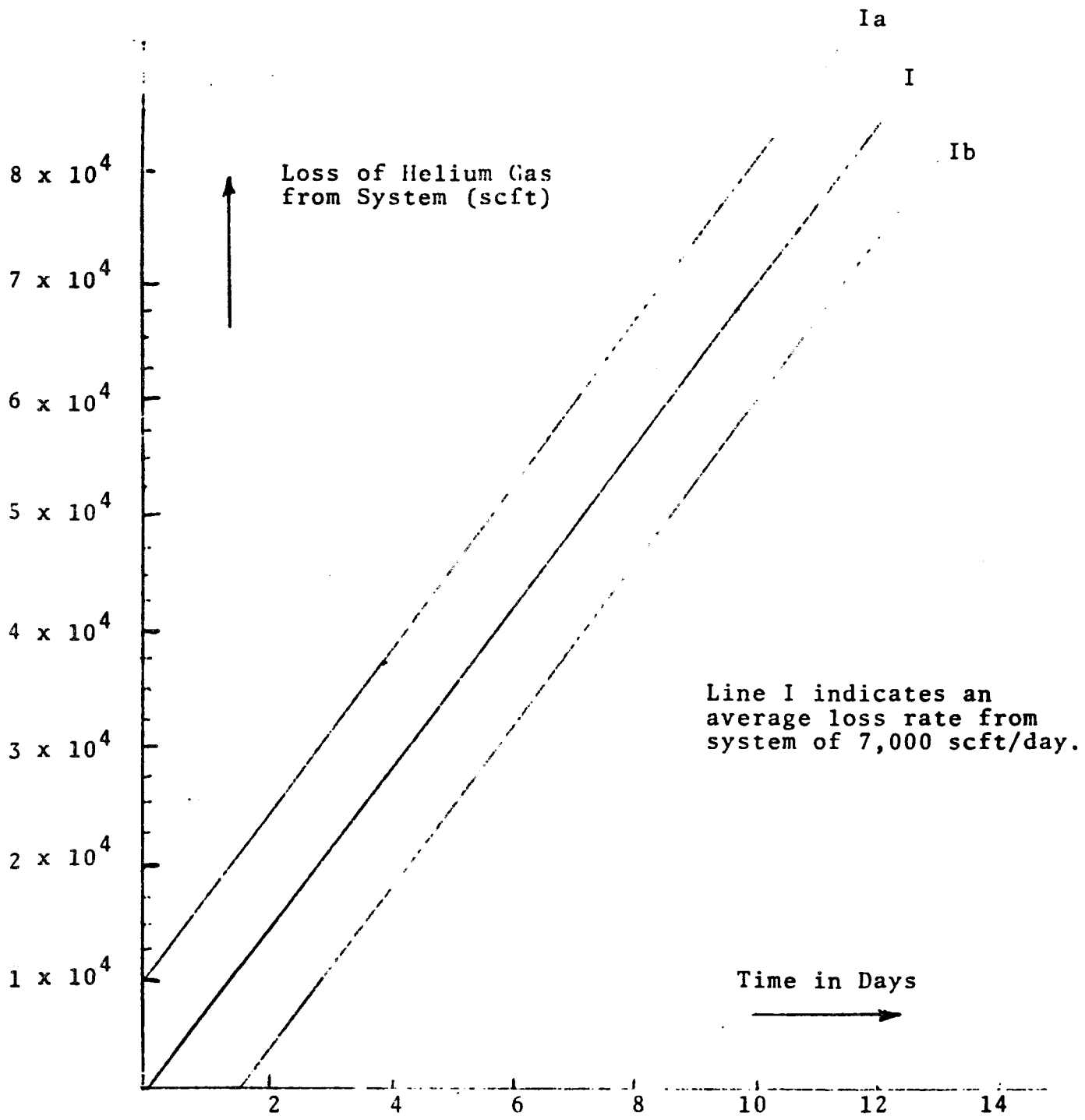


FIGURE 4

THE CENTRAL HELIUM LIQUEFIER

I. Introduction

a. Relationship to the Overall Refrigeration System:

The refrigeration system of the Energy Doubler consists of several parts which work together for maximum output. The various parts can also work independently to carry a reduced load. The major components which contribute to the refrigeration are as follows:

1. The nitrogen refrigerator, with dewar.
2. The Central Helium Liquefier, with dewar, pump, and subcooler.
3. The Satellite refrigerators, with assorted transfer lines and subcoolers.

The nitrogen reliquefier will produce 50 tons of liquid nitrogen per day into the 14,000 gallon dewar. It is operating in a closed cycle and collects warm nitrogen gas from the magnet shields, the transfer lines, the helium cold box, purifiers, and satellites. The liquid will be transported in vacuum insulated transfer lines from the dewar to all use points.

Liquid helium from the Central Liquefier will be collected in a 5000 gallon dewar and pumped to each of the 24 satellites and subsequently distributed to the ring. Each satellite will use 111 liters for lead cooling and satellite "boosting". The boosting action results in 690 watts

of 4.9°K refrigeration being delivered to the magnet string and the 111 liters from the Central being warmed to ambient temperature and recompressed for delivery back to the Central and use in the high pressure stream to the cold box.

This system has the advantage of extracting the available refrigeration from the stream at the satellite location, reducing the size and cost of the necessary transfer lines.

b. General Equipment Plan:

The equipment consists of a mixture of reconditioned Air Force surplus and newly designed and purchased components. Figure 1 shows the layout of the major components in the new 50 ft x 130 ft building which is equipped with a five ton crane. The following equipment is located inside the building (numbered as in Figure 1):

1. Two 4000 hp surplus air compressors which have been reconditioned, restaged, and converted to helium service.
2. One similar compressor in process of being prepared for future service in a nitrogen reliquefier.
3. Three 4000 hp synchronous motors for these compressors (also surplus).
4. 4 kV switchgear and solid state field supplies.
5. Helium refrigerator cold box, 4875 liters/hour.
6. Local valve and instrument cabinet for refrigerator.
7. Two level control room structure.
8. Motor control center for auxiliary motors.
9. Oil removal system.
10. Seal gas cleanup system.

The following equipment is located outside:

11. 15MW transformer for main motors and 1.5MW substation for utility power.
12. Air cooled heat exchangers.
13. Cold box for nitrogen refrigerator.
14. 14,000 gallon liquid nitrogen storage vessel.
15. 5,000 gallon liquid helium storage vessel.
16. 30,000 gallon gas storage vessel rated at 250 psig.

II. Interior Structures

- a. Compressor Foundations: To be assured of a successful compressor operation, it is necessary to build adequate mountings for them. The compressors which we are using weigh 185,000 lb each, plus another 50,000 lb for the motors. Since the machines are reciprocating and have large cylinders (see specifications), substantial shaking forces are developed by the 277 revolutions per minute of the motors. Typical shaking forces are about 10,000 lb and couples are about 130,000 ft lb.

The foundations were designed by Dames and Moore. Figure 2 shows a sketch of the model which they used for computer analysis. The main support is a 3 ft thick reinforced slab, 90 ft long and 35 ft wide. The top of this slab was at normal floor level. The main crankshaft frames were elevated 54 inches to permit bringing suction pipes in the bottom of the cylinders without the use of pits, underground piping, and other complications. This foundation was separated from the building floor around it by soft padding. The pad was supported on 60 piles driven to a depth of about 36 ft and a loading of 30 tons each. The

piles were 12-3/4 inches in diameter with 3/8 inch walls and were filled with concrete.

The total amplitude of vibration expected is less than .003 inches. This amplitude is expected to be noticeable, but not troublesome to persons or machinery.

- b. Cold Box Pit: A steel-lined pit 13 ft in diameter and 36 ft deep was constructed under the helium liquefier. This was necessary to permit the assembly of the various components of the cold box and to make it possible to make repairs in the future with a minimum of delay and expense.

- c. Control Room Enclosure: This is a two story prefabricated industrial office type structure. It is 20 ft wide by 40 ft long. The lower level serves as a maintenance and storage area and contains the gas analysis equipment and the sanitary facilities. The upper level houses the control consoles and all of the remote readout and automatic logic. It also has space allotted to prints and records. The upper level is designed to provide convenient access and view downward toward the compressor system, on the second level to the cold box maintenance valves, and upward to the third level platforms which permit access to the valve operators, transfer lines, and turbines on top of the cold box.

III. Helium Compressors

a. Compressor Redesign: The redesign of the seals and the flow calculations were performed by Commercial Machine Works, using standard techniques, as well as the shop work and assembly of the compressors.

1. Introduction

Two Worthington six cylinder, 4000 hp reciprocating air compressors were reviewed for determination of performance characteristics when applied to helium service. Several alternates were considered in an effort to obtain a flow rate and hp usage consistent with the system requirements and compressor capability.

2. Design Criteria

Existing compressors are five stage, six cylinder units as follows:

First stage	-	34-1/4inch	2 cylinders
Second stage	-	27 inch	
Third stage	-	15 inch	
Fourth stage	-	9 inch	
Fifth stage	-	6 inch	

New design conditions call for a three stage application. Therefore, performance of existing cylinders has been reviewed and based on this requirement, initial inlet pressure of 15.435 psia and final discharge pressure of 180.81 psia are the parameters of the design review. Effort has been made to maximize the mass flow through the unit, requiring consideration of different cylinder and interstage pressure arrangements.

Four basic alternate design criteria were evaluated. The option selected was to utilize all existing compressor cylinders with adjusted interstage pressures to allow maximum mass flow throughput. The crank end of one first stage cylinder is unloaded. The 15 inch, 9 inch, and 6 inch cylinders operate in parallel as the third stage of compression.

3. Performance

The unit is expected to perform as shown in the Table below:

TABLE I
UNIT PERFORMANCE

<u>Item</u>	<u>Stage of Compression</u>		
	<u>1</u>	<u>2</u>	<u>3</u>
Cylinders used	2-34-1/4"	1-27"	1-15", 1-9", 1-6"
Type of gas	Helium		
Piston displacement-cfm	7903	3268	1441.3
Compressor speed-rpm	277		
Altitude	Sea level		
Intake temperature-F	80	100	100
Intake pressure-psia	15.435	38.57	87.97
Discharge pressure-psia	39.337	89.73	180.81
Discharge temp.-F	325	325	287
Volumetric efficiency-%	84.88	85.28	84.95
Actual capacity-cfm	6708	2787	1224.4
Equivalent capacity #/hr - dry	4286.5	4286.5	4286.5
Bhp/stage	610.7	536.3	501.8
Total	1648.9		

Notes: Frame and shaft loading changes resulting from the new design conditions are not of a significant order of magnitude, therefore, no modification or changes in original cylinder configuration is required.

Shaking forces will be the same as the original design values.

First stage discharge pressure should not exceed 40-41 psia.

b. Compressor Modifications

1. Introduction

Compressor component and cylinder modifications required to adapt this air unit to helium service are outlined in detail showing both the physical and material changes required.

Other repair and/or replacement requirements were covered under a separate contract. All installation and alignment work has been completed. The compressors are fully grouted and mounted with special tiedown bolts. Extensive motor rework has also been completed, including testing, new windings as required, re-insulating, new bearings, installation and grouting.

2. Compressor Valves - Feather

All feather valves have been rebuilt using new valve strips.

The following work has been performed:

Grind and lap valve seats.

Grind guard to reduce lift.

3. Compressor Valves - Plate

All plate valves were rebuilt using new wear components as indicated. Valve lift was reduced for helium service.

The following work has been performed:

Grind and lap valve seats.

Replace plate springs and provide glass-filled Teflon buttons for springs.

4. Valve Types

The cylinders are equipped with feather or plate valves of various sizes as shown in Table II.

TABLE II

NUMBER AND VALVE TYPE PER CYLINDER

<u>Stage</u>	<u>Quantity</u>	<u>Size</u>	<u>Type</u>
First	12	13"	Feather
First	12	13"	Feather
Second	20	8-1/2"	Feather
Third (15")	12	6-1/2"	Plate
Third (9")	8	5-1/4"	Plate
Third (6")	8	4-1/4"	Plate

5. Piston Rider Rings

All pistons were modified to accept graphite-carbon-filled Teflon rider rings, Compressor Products Type FOF31 or approved equal.

Rider rings are solid, uncut type prestretched for installation. Two rings per piston.

Rider ring projection is .050". Piston o.d. have been turned where required.

Remachining of the babit rider rings in the ring carrier for replacement by Teflon rider rings was not successful for the first stage 34-1/2 inch pistons due to previous modifications and repairs in this area.

All new first stage cast iron ring carriers were machined to fit.

6. Piston Compression Rings

All pistons are equipped with carbon-graphite-filled Teflon rings, Compressor Products Type FOF31 or approved equal. First and second stage rings are one piece angle cut with contained stainless steel expansion ring. All other rings are one piece angle cut, no expansion ring required.

7. Number of Rings Per Piston

First stage	2
Second stage	2
Third stage (15")	4
Third stage (9")	5
Third stage (6")	6*

*Piston machined with eight grooves. Center two grooves will not be required. No modification necessary.

8. Piston Rods

All piston rods were ground to a common diameter in the packing area. It was necessary to remove .020" of stock to attain cleanup at common diameter. Two rods were replaced. A 12-15 microinch finish was used.

9. Piston Rod Packing

New packing cases and packing were furnished with provision for oil and vent connection.

First and second stage packing has a minimum of five rings, Compressor Products Type 114-5, or approved

equal using Type FOF-31 material with lapped bronze backup rings.

10. Distance Piece

A new oil scraper gland seal was added to prevent helium leakage into crank case. The unit seals in both directions and is specified as Compressor Products Type 140.

Access openings on each distance piece were enclosed, with covers of 3/4 inch steel plate.

Existing lube oil and vent connections on distance piece housing were used in making all internal connections.

11. Cylinders

All cylinders were final honed to produce a 15-18 micro-inch finish.

12. Gaskets

Garlock Type 7021 gaskets were used throughout.

IV. Piping and Flow Systems

- a. Compressor Piping: The entire piping system for both helium compressors has been completed. The instrumentation and valve control systems are also in place. A portion of the piping to the cold box is still in progress, but the compressors are essentially ready to run and require only the final check of the switchgear. Figure 3 shows the gas management system for one compressor.

October 20, 1978

XIV. CONTROL SYSTEM FACILITIES

M. F. Gormley

The control system planned for the Energy Doubler/Saver would represent a melding of new facilities (offered by modern technology) with a distillation, based upon experience, of the facilities that have been found to be necessary, desirable or useful in existing subsystems of the accelerator. In addition to providing a communications scheme for monitoring and setting devices distributed around the four mile circumference of the ring, the existing control system provides a variety of facilities: a Clock System for synchronizing events relative to significant times in the accelerator cycle, an Abort System for allowing a detector (at any location in the ring) a method of informing the abort magnet power supply that the beam should be dumped, a Current-Regulation System for the ring magnet power supplies, and a Data Collection and Control Facility for diagnostic and tuning purposes and for keeping the operator in the control room informed. With the exception of the power supply regulation system (which is discussed elsewhere) a description of the Doubler control facilities is presented in the following paragraphs.

A. Doubler Clock System

A new, dedicated transmission cable, which runs from service building to service building around the ring, is used to synchronize devices scattered around the ring with the Doubler cycle and to synchronize the Doubler itself with the Main Ring and/or Booster.

The transmission cable carries the output of a free running, bipolar, one megahertz oscillator onto which a number of reference times (start of Doubler ramp, beginning of Doubler flat-top, etc.) have been encoded in the form of phase reversals. The reference times together with the oscillator are typically used to provide trigger pulses to digital electronics such as waveform generators. The one megahertz oscillator fixes the timing resolution of the trigger pulses at one microsecond, which is adequate for almost all devices. The number of distinct references and the range of the Doubler clock would initially be chosen as eight references and one hundred twenty-eight seconds, respectively, which should be adequate for accommodating most complex operating modes with widely different cycle times. This type of clock system represents a straightforward extension of the timing and synchronization facilities used throughout the existing accelerator subsystems.

B. Doubler Abort System

A means for dumping the beam quickly, upon detection of a potentially hazardous situation (e.g., a quench), will be required for Doubler operation. A new, dedicated transmission cable around the ring together with an abort-input-panel in each service building is needed to provide this facility. The abort-input-panels would receive triggers from devices (loss monitors, etc.) which detect the potentially hazardous condition; the transmission cable is used to convey the information from the service building to the abort magnet power supply as quickly as possible. Typically, the delay time in transmitting the firing pulse from the worst-case service building to the abort magnet power supply is 100 microseconds--a delay which is ordinarily negligible in comparison with the rise

time of the abort magnet. This scheme for communicating the firing pulse to the abort magnet power supply represents a straightforward extension of the existing main ring abort system. For the Doubler abort system either one or two new transmission cables will be required, depending upon the details of the dump(s) for clockwise and counter-clockwise acceleration.

C. Doubler Data Collection and Control Facilities

The amount of hardware and software required to support an accelerator as large as the Doubler is expected to be comparable to that of the existing Main Ring. Control system electronics (vacuum readout electronics, timing channel outputs, correction element power supply controllers, etc.) will be located in relay racks at each service building. Serial communications facilities, providing both programmed input/output and high-speed block transfer capabilities, will be supported with new transmission line cables which connect the control room and Cross Gallery with the service buildings. A single front-end mini-computer, located in the Cross Gallery, is used to manage and coordinate the communications links.

The control station electronics located in each service building make use of a standard, parallel-bus structure provided by a CAMAC crate (IEEE-583). An extensive repertoire of interface electronics for this bus structure is available off-the-shelf. Provisions for three types of distributed intelligence facility are accommodated at the service building control stations: (1) intelligent modules, supported off the CAMAC crate, which would, for example, generate waveforms or provide simple, dedicated closed-loop control, (2) a portable, intelligent terminal which connects into the CAMAC crate and provides local diagnostic and display facilities and (3) an

intelligent, dual-ported crate controller which allows one to trade off a large fraction of the conventional monitoring from the host computer system. These three varieties of distributed intelligence, which are available and supported within the structure of the existing control system, are made possible by the products of Large Scale Integration in the form of microprocessors. Since faster, cheaper and more powerful LSI components will become available during the development and construction of the Doubler, it will be attractive to rely more heavily on the types of distributed intelligence discussed above.

The incorporation of the Doubler's control needs into the existing control system would be quite difficult unless the structure of the existing system were reorganized and the processing power of the existing system were enhanced. A computer acquisition project which would provide such reorganization and enhancement is currently scheduled and budgeted for FY80 under Accelerator Improvement Projects. During FY79 the major controls effort relative to the Doubler will be construction and installation of the facilities to be used in conjunction with the sector test. New transmission line cables have recently been installed around the ring to support these facilities. CAMAC crates and interface electronics are installed in Service Building A1. Future growth is expected to proceed in parallel with the installation of magnets in the tunnel.

IV. FERMI LAB DOUBLER MAGNET DESIGN AND FABRICATION TECHNIQUES

K. Koepeke, G. Kalbfleisch, W. Hanson, A. Tollestrup, J. O'Meara, J. Saarivirta*

ABSTRACT

During the last year, the Fermilab Doubler magnets have benefited from a development effort to upgrade the performance of the superconducting magnets. This paper presents the results of this effort. The design philosophy and the fabrication techniques used on current magnets will be discussed, along with innovative laminated tooling which has been designed to give Fermilab a two dipole a day production capability. Specific topics to be discussed are coil geometry, coil winding techniques, coil clamp collars, buss geometry and insulation, integral quench heaters for quench protection, coil twist, coil helium irrigation and assembly techniques that assure azimuthal preload and accurate coil size.

INTRODUCTION

In order to minimize the construction and operation cost of the Fermilab Energy Doubler project and also due to space limitations in the existing 500 Gev synchrotron tunnel, a relatively simple "warm" iron, cold bore magnet design¹ was adopted. Three distinct modules are separately fabricated and assembled to form a complete magnet: the collared coil, the cryostat and the iron shield yoke.

The coil package for the dipole consists of a two-shell design with the first 10 turns of the inner shell at the ends separated with .100" spacers to reduce the peak field at these locations. By varying the azimuthal coil angles of the inner and outer shell, the two-dimensional field region can be adjusted to cancel the sextapole and decapole terms present in the ends of the magnet.

By virtue of its location between the rigid coil clamp collar and the iron yoke, the cryostat need not be self-supporting and is fabricated out of thin stainless steel sheet metal. Precise alignment of the collared coil assembly relative to the iron yoke is assured by means of rigid G-10 force transfer blocks located periodically within the cryostat. The cryostats come partially assembled from several vendors.

The magnetic shield differs from conventional magnet yokes only in their cross section. They are assembled out of laminations into left and right halves in a stacking fixture and joined around the coil and cryostat assembly to complete the magnet.

Over 100 collared dipole assemblies have been completed. Roughly half of these have been inserted in cryostats with iron shields and are in various stages of installation in the synchrotron tunnel. As problems became evident during their construction and testing, they were corrected or improved. Laminated tooling was designed to improve coil accuracy and production rate. Coil measuring fixtures were constructed to monitor coil sizes. Conductor motions have been reduced with increased preload. A new type 5 coil clamp collar has been adopted which has a higher resistance to fatigue and is torsionally more rigid. Heaters have been installed in the dipole for quench protection and a new buss geometry has been adopted.

Manuscript received September 28, 1978.

*Fermi National Accelerator Laboratory, P.O. Box 500, Batavia, Illinois 60510, operated by Universities Research Association, Inc. under contract with the U.S. Department of Energy.

The prototype Doubler quadrupole magnet was a "warm" iron, cold bore, three-shell design. Seven magnets of this type have been constructed and successfully tested. Recently, a two-shell quadrupole design was adopted to simplify fabrication and allow a higher production rate.

COIL FABRICATION AND MAGNET ASSEMBLY

The sequence of fabricating a collared dipole coil assembly starts with the winding and hot molding of two identical 35 turn inner coils. Our original technique of "saddle" winding these coils was abandoned in favor of our "pancake" technique. This technique consists of winding a flat coil around an articulated key mounted on a .060" steel retainer sheet. After winding, the coil is covered with a second .060" steel retainer and transversely compressed by means of side rails to a dimension approximately equal to the desired outer arc length of the finished coil. The side rails are then fastened to the retainer sheets, resulting in a "pancake sandwich". This is forced around a mandrel using a female mold in a 22' long press and cured, yielding the conventional "saddle" coil configuration. This technique has proved to be fast and accurate.

The outer coils are "saddle" wound using the inner preformed coils as a winding mandrel. This technique has resulted in adequate conductor placement accuracy due to the smaller number of turns (21) in the coil. In order to provide for LHe edge cooling, a layer of .021" thick interrupted G-10 is placed between the inner and outer coils.

The cured two-shelled upper and lower coil halves are placed on the assembly mandrel, covered with .030" thick pre-molded mylar ground insulation (later to be Kapton) and fitted with 4" long collar sections. The loosely collared coil assembly is placed into a pair of massive channel-shaped fixtures which provide precise vertical and horizontal constraints to the collar as it is sized in a 3200 ton hydraulic press. Finally, the assembly mandrel is removed from the coil by means of a ratcheted-action hydraulic cylinder and the collar is welded on both sides by automatic welding machines.

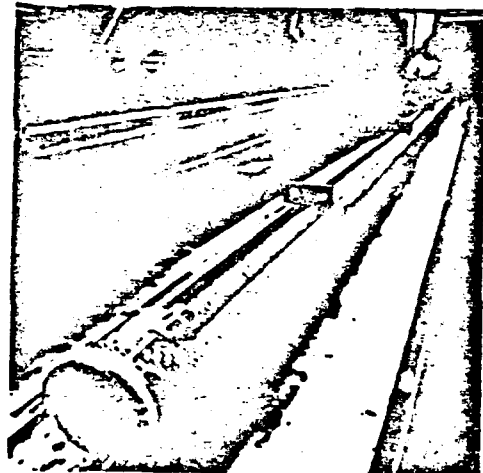


Fig. 1 Dipole lower coil

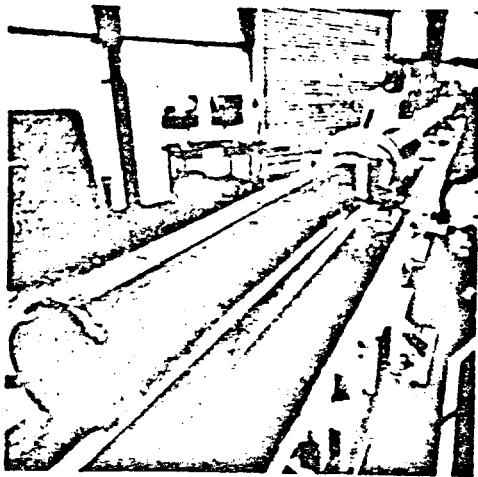


Fig. 2 Collared dipole coil half inserted in cryostat

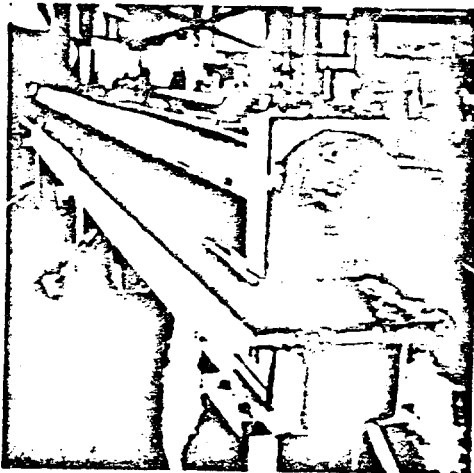


Fig. 3 Half yoked dipole

A magnet is completed by pushing a collared coil into a prefabricated cryostat, welding on the cryostat end closure pieces and finally fitting the two halves of the prefabricated yoke. Note that this production sequence lends itself to production line techniques. With the present manpower available, a production rate of 5 collared coils per week has been achieved with 250 manhours required per collared coil. The in house manpower per magnet is approximately 400 manhours if we add the cryostat, yoke and inspection steps. It is expected that the production rate can be doubled with the efficient use of available tooling and three fully staffed shifts.

The quadrupole magnet fabrication utilizes the same principles devised in the dipole development program except that the coils are all saddle wound. The four sets of coils are wound as double shells, pressed and cured in the same manner as the dipoles. In order to support the four individual coils, the collars are applied from four sides rather than two, necessitating the application of collars one at a time.

TOOLING

The equipment available to produce collared dipole coil assemblies consists of three 22' long winding machines for producing coils, two 22' long presses with

integral molds for forming coils and two 3200 ton presses for sizing and welding collared coils. In addition, there exist several sets of inner and outer winding mandrels, assembly mandrels, and channel tooling used to size the collars.

All molds, winding mandrels and keys presently in use are made of laminations. In our experience, 22' long tools, even in simple shapes, cannot be economically made to a .0005" tolerance. However, relatively inexpensive dies using Elox cutting techniques can produce complex cross sections to .0005" tolerances and a lamination uniformity of .0001" is within the present state of the art. Tools assembled out of stacked laminations are therefore uniform thru-out their length and make replication of tooling very simple.

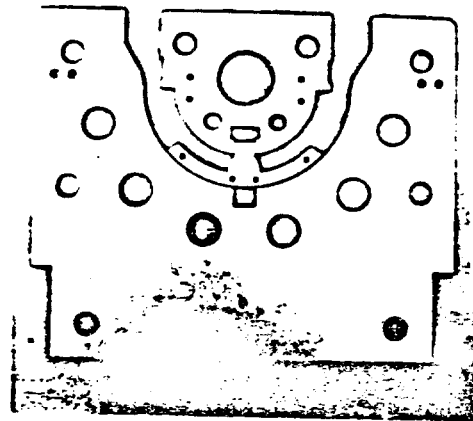


Fig. 4 Outer dipole mold laminations

To achieve these tolerances, the laminations are made out of mild steel. All bearing surfaces of the tooling are therefore fitted with hardened steel inserts of simple rectangular cross section which can be ground to a .0005" tolerance. These inserts also allow us to change the molded azimuthal angles of subsequent coils to compensate for systematic field errors measured in completed magnets.

CONDUCTOR PLACEMENT ACCURACY

In order to reduce the AC loss inherent in ramped magnets, the superconducting cable adopted for the Doubler magnets was a Rutherford type cable made by twisting 23 strands, each of .027" diameter, into a (.044" - .055") x .307" keystone cross section in a Turkshead die. The keystone shape allows for proper conductor stacking in the cylindrical coil geometry and is porous to allow for LHe irrigation. The porosity of coils is maintained by the use of a non-adhesive 7/12 lap layer of .001" x .375" Kapton for electrical insulation followed by a .125" gap helical wrap of .007" x .25" B-stage epoxy impregnated glass tape for bonding.

The typical mean azimuthal arc length vs. applied pressure behavior of a dipole inner coil is plotted in Fig. 5. Rigid and accurate conductor placement of these porous coils is obtained by compacting the coils during assembly into a split collar. The collar presents a rigid, precise radial and azimuthal outer boundary to the coils.

To the extent that the coils act like piece

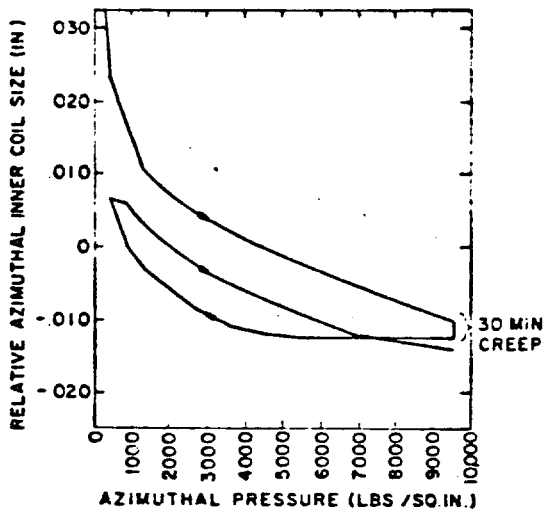


Fig. 5 Inner dipole coil size measured relative to 2.145", the mold dimension.

wise linear springs in the azimuthal direction, the upper to lower coil boundary within the collar at a given azimuthal force is determined by half the difference in azimuthal coil size measured at that force. These coil sizes (Fig. 6) are regularly measured as part of our ongoing quality control program. Although the coil sizes vary within a .020" range, resulting in a variable preload, the coil boundaries for collared coils are on the average within .001" of their calculated position.

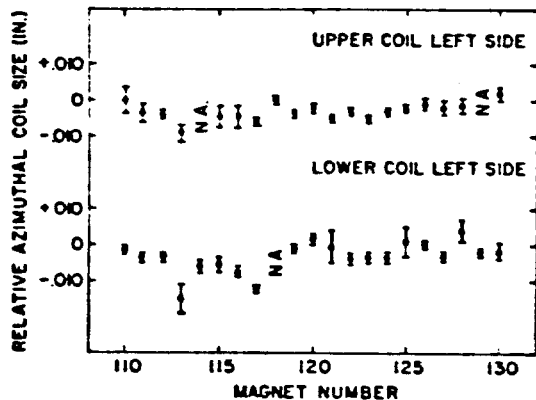


Fig. 6 The inner dipole coils were measured at an azimuthal pressure of 4780 lbs./sq. in. The error bars represent the standard deviation of 11 measurements taken along the length of the coil.

The bore dimension of the magnet is determined by the wall thickness of the coils, which reproduce within .001" due to the small cumulative tolerance in this direction. Strain gauge measurements on the OD of the collar and the ID (bore) of the coils have shown that the radial compression of the coils is less

than .001".

The azimuthal conductor placement within individual coils is harder to control. The conductor distribution within the inner dipole layer, the layer whose conductor distribution is most difficult to control, has been optically measured on cross sections of collared dipoles. The measurements indicate that the conductors have a mean position error relative to the correct position of less than .001" with a standard deviation of .003". For the outer dipole coils and the quadrupole coils, this error is expected to be less due to the smaller number of conductors present.

Calculations and measurements indicate that the conductor placement of the magnet ends are an order of magnitude less critical than the two dimensional part of the magnet. In this case, the contour of the ends is assured by molding precision G-10 spacers to the ends during the coil curing stage. These spacers remain with the coil during assembly.

CONDUCTOR MOTION AND PRELOAD

Measurements² performed on 1 ft. long prototypes of the Doubler superconducting dipoles indicated that the azimuthal compaction of coils in energized magnets can be limited to a few thousandths of an inch with adequate azimuthal preload. Early attempts to size coils such that this preload is trapped in the collar on full sized magnets failed for the following reasons: The coil clamp collar used to be bonded at 200°F with heat cure epoxy. During this process, the trapped coils under the combined effect of heat and pressure collapsed. This effect has been measured to start at 125°F.

The preload that remained was further reduced by the differential coil to collar shrinkage from room to LHe temperature. The difference in azimuthal coil size $\Delta l(P)$ measured at room temperature and LN temperature both at azimuthal pressure P has been measured to follow the equation:

$$\frac{\Delta l(P)}{l} \bigg|_{\substack{300^{\circ}\text{K} \\ 78^{\circ}\text{K}}} = (3.55 \pm .35) \times 10^{-3} - (2.3 \pm .22) \times 10^{-7} (P - P_0) \quad (\text{Eq. 1})$$

where P_0 equals the pressure at which the sample is cooled. All pressures are expressed in lbs./sq. in. The $(P - P_0)$ term accounts for the difference in Young's modulus at the two temperatures.

In order to assure adequate preload, the inner and outer coils of the superconducting dipole have to be molded .040" and .005" oversize in the azimuthal direction. The collars are now welded to eliminate temperature induced coil yielding. Upon cool down, at least 4700 lbs./sq. in. of azimuthal preload remains in the inner coil. This has been verified by slitting the collar at the median plane of the dipole and measuring the force required to return the sprung collar back to its nominal dimension at room temperature and LN temperature.

Conductor motion in the superconducting dipoles has been limited to less than .003" in both the azimuthal and radial direction at 45 KG. The axial motion at this field has been measured for E22-43 and equals .050". The motion related field perturbations as a function of current are therefore dominated by the two-dimensional part of the magnet.

COLLARS

Fatigue tests performed on 1" sections of the type 4 collar previously used on the dipoles predicted

their failure after 10 magnet cycles. Furthermore, the collar was unable to contain the coil preload without excessive deformation and had insufficient resistance to axial torques.

A new "solid" type 5 collar design has been adopted that overcomes these problems. The fatigue point has been raised to 10^7 cycles, an order of magnitude greater than the anticipated life of the accelerator. Any twist present in the collared coil assembly after welding is measured relative to a surface plate and reduced to less than 3 milliradians with a torque fixture. The collar is then surface coated in place with low viscosity room cure epoxy. It penetrates .1" and effectively results in a tube of this wall thickness to counteract any torques present.

COIL FATIGUE

The premature failure of the type 4 collar under repeated small motions prompted a test of the inner dipole coil under similar conditions. The cyclical azimuthal pressure and the resultant conductor motion that the coil experiences during a magnet current cycle was approximated by applying an azimuthal variable pressure at a rate of 2 cycles per second. The test was performed with the sample immersed in LN. A comparison of the azimuthal coil size measured at the start of the test and after the sample experienced 10^6 pressure cycles showed no measurable size reduction or any other visible signs of damage.

BUSS LEAD

Unlike the other conductors in the magnet, the buss electrical insulation has to withstand 3 KV. To obtain the radial clearance in the magnet for the additional insulation, the buss cable was fashioned out of undersized .025" diameter strands to a cross section of (.043" - .049") x .286". This buss is insulated with 4 layers of 7/12 lap .001" x .375" Kapton followed by an armor layer composed of alternating dry and B-stage impregnated .007" x .25" Kevlar tape helically wrapped with a butt lap.

HEATERS

Two heaters, one redundant, have been installed in the dipoles as part of a proposed quench protection circuit for the Doubler. The purpose of the heaters is to initiate a uniform longitudinal quench in the superconducting turn immediately adjacent to the heater. This quench rapidly propagates in the transverse direction from turn to turn, permitting the magnet to absorb its stored energy without damage.

Each heater consists of a .005" x .200" stainless steel strip wound under the glass tape of the complete first turn of an outer coil. It faces away from the coil and is insulated from the turn by a .010" strip of Kapton.

QA QUADRUPOLES

The prototype QA quadrupole was a 3.25" bore, 3-shell design. The tooling for this magnet was designed for accuracy and sufficient preloading capability, both of which were attained.

The first several quads did not attain a preload internally. The loss of preload was traced to the heat cure cycle of bonding the collars. The last two quads were then bonded with room temperature cure epoxy. They did achieve azimuthal preload. The verification of preload was obtained by magnetic field measurements under excitation. The 12-pole

component is sensitive to change in the coil size. By calculation, the ratio of the 12-pole to the 4-pole component (i.e. quadrupole) at 1 inch radius changes by 1 part in 10,000 for a 0.001 inch azimuthal squeeze. Adequately preloaded coils will then show a constant 12-pole ratio with varying excitation current; a change will indicate motion. The heat cured collared assemblies show a 12-pole ratio changing with excitation (Fig. 7A). The magnitude of the observed change in this ratio agrees well with independent mechanical measurements of the coil motion under excitation. The room temperature cured collared assemblies (Fig. 7B) show a constant value for this ratio, indicating a motion of less than 0.001".

QB QUADRUPOLE

The production QB quadrupole is a 3.5" bore, two-shell design. Dipole tooling techniques have been incorporated to produce tooling that will allow a high production rate. A spacer has been incorporated in the inner coil which reduces the 20-pole a factor of 5 over the QA design. The first QB magnet tested reached 5-00 A (22KG/in.) in three quenches. A preliminary harmonic probe analysis indicates no conductor motion in the coils.

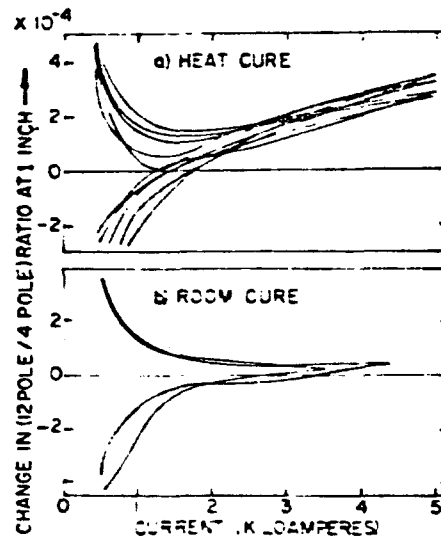


Fig. 7 QBA Magnet 12 Pole to 4 Pole Ratios.

ACKNOWLEDGEMENT

The teamwork of the Fermilab staff is responsible for the success of the Doubler magnet production program. The authors wish to specifically acknowledge the contribution of S. Barath, J. Carson, J. Humbert, J. Jagger, G. Jugenitz, D. Smith and the remaining staff of the Fermilab Magnet Facility.

References

1. P. Livdahl, IEEE, Trans. Nucl. Sci., NS-24, No. 3, 1219 (1977)
2. A. Tollestrup, et. al., IEEE, Trans. Nucl. Sci., NS-24, No. 3, 1331 (1977)

Alvin V. Tollestrup

I. INTRODUCTION

This report will update the Progress made on the Fermilab Energy Doubler/Saver. Since the last report made to this Conference in 1976, over 100 22 foot long coils have been constructed and studied. About 50 complete magnets have been constructed in the Magnet Fabrication Facility by techniques that routinely turn out 5 magnets/week and can be easily expanded to 8/week. The tooling is such that it can be easily duplicated.

A quadrupole has been developed and tested using the same mass production techniques as are used for the dipole, and a production line to produce it is currently coming into operation.

A string of twenty-five magnets have been installed in the Main Ring tunnel and is undergoing cryogenic tests and beam transport tests at 100 GeV.

Three satellite refrigerators for the first sextant of the machine are installed and being tested and the Main Refrigeration plant is 80% complete and will be brought on-line in 1979.

Finally, a Magnet Test Facility has been constructed using a 1500 watt refrigerator that has six stations available for cooling and testing complete magnets. This facility will be able to provide complete tests of both the field quality and the cryostat, before each magnet is installed.

This report will try to provide an overall description of the progress made, and the individual reports that follow will give more complete details.

II. DIPOLE PROGRAM

The dipole for the Energy Doubler/Saver is 22 feet long, has a central field of 42.5kG, stores .5 mega joule of energy at full field, and has a useful field region that is approximately $\pm 1"$ about the axis. A cross section is shown in Figure 1. The main thrust of the development program has been to find means to construct these dipoles inexpensively and accurately. Hence, there was never any effort to construct one or two models very carefully using highly skilled labor to verify the magnetic field quality. Since Maxwell has provided the means to calculate the field shape (there is no saturated iron anywhere in the magnet), the problem is simply to get the conductors in the correct position. At first it was thought that the conductors would have to be placed correctly to about $\pm .001"$. However, a new philosophy has developed from our experience.

First, tooling has been developed that makes the coils in a highly reproducible geometry. Measurement of the completed coil then discloses errors in the geometry. These errors are used to correct the shape of the subsequently produced coils by small changes in the angles of the current blocks. This process converges rapidly and the "noise" in the manufacturing process then determines the field quality. It is the reduction of this noise to a minimum, while retaining inexpensive mass production techniques that has been

the goal of the magnet development program. The magnets produced in the early stages, which are not of "machine quality", have been used for system tests of cryogenics and for development of a suitable power supply that can both power the magnets at 4500 Amps as well as protect them in case of quenches. These developmental magnets are also suitable for use in the external beam lines.

Coil Fabrication

The coils consist of two layers as seen in Fig. 1. The angles of the current blocks are such that the good field region is maximized. The coil is manufactured in the following fashion. Cable, as received from industrial sources, has been double wrapped with .001" Kapton film over which is spiral wrapped a glass tape that has been impregnated with 8-Stage epoxy. The insulation is tested at 1,000 volts as the coil is manufactured. The inner coil is wound around a precision inner key as a flat "pancake" between two thin sheets of .030" iron. The assembly is then placed in a 22' long 1,000 ton press and the coil is forced into a precision mold, heated and cured under pressure.

The intermediate "banding", which is G-10 strips with slots in between to allow helium to percolate through the coils, is then put in place. The outer coil is now wound using the inner as a winding mandrel. Finally, this entire package is again placed in a precision mold 22' long situated in a 1,000 ton press, and is heated and cured under pressure. This then completes a "half coil".

The second half coil is formed in the same fashion except that 1/2 turn of the outer winding is left out and instead a single conductor is molded into the last 1/2 turn of the outer coil at the parting plane. This conductor forms the "return bus" for the current in a string of magnets. Each magnet has two leads at its upstream end and two at its downstream end. This allows the magnets to be connected in series without the necessity of a warm-cold current lead transition or the complication of a cold distribution bus system. A more complete discussion of coil fabrication is given in paper JC-4.

Support Structure

Two half coils are then assembled together, covered with a triple overlap of 0.010 in Mylar (to be changed to Kapton for radiation resistance) and placed inside precision stamped stainless steel "collars". These interlocking collars furnish the main support skeleton to contain the large magnetic forces. For instance, a conductor typically has nearly 100 lbs. per inch of magnetic force which must be sustained by the support system.

The collaring system is a major innovation. The pieces are inexpensive, can be mass produced with high accuracy (tolerances of the order of a few tenths of a mil) and their interlocking nature makes them very strong and easy to assemble by halves. After a loose assembly is made, the coil and collars are placed in a third 1,000 ton press. Precision support pieces push the collars completely together. This requires a force of about 5,000 lb/in. of length due to the fact that the coils are larger than the collars. The system is elastically compressed until the collars are closed at which point they are welded with three welds along the interlocking fingers on

each side. The compression is sufficient so that the mechanical forces from the collars exceed the magnet forces. This was a difficult problem to solve due to the contraction of the coil being more than the collars during cool down. This problem was solved by very carefully adjusting the size to which the coils were molded, as well as the mold temperature and pressure. It is found that any heating of the coil above 50°C causes the relaxation of this preload. The fact that this problem is solved is attested to by both magnetic measurements of the multipole moments as a function of current as well as direct measurement of the coil motion during excitation. Finally, the coil is placed on a flat table and measured for twist. After straightening, the collars are painted with room cure epoxy which makes the structure much more rigid in torsion and locks adjacent collar laminations together.

Extensive calculations and measurements have been made of the deflections and stress levels in the collars. The results may be found in Paper JC-4. Fatigue tests made at 80K show the collars should survive over 10 cycles.

The coil at this point is ready for the cryostat. The winding and collaring operations have required 250 man hours. Over 80 of these coils have been given vertical dewar tests at this stage where training, ramp rate dependence, deflections, and quench behavior are studied. This program is a research effort only and will not be necessary for every magnet.

Cryostat

The cryostats are partially assembled and tested in the plants of external fabricators. The coil is inserted into its cryostat and at several points vacuum and electrical insulation tests are carried out. The final assembly is leak tight among the five separate compartments - beam tube, single phase helium, two phase return helium, N₂ intermediate shield, and insulating vacuum - to a level of 2×10^{-10} atm cc/sec (helium) torr. liter/sec. The coil is tested for electrical breakdown at 3,000V. See paper CA-13.

Yoke

Finally, the cryostat and coil assembly are placed in the iron flux return yoke. The yoke is carefully measured and fit to the cryostat since the basic centering forces for the coil must come from the yoke. The support pieces are G-10 and there are 9 stations per magnet providing an elastic restoring force constant of 125 lb./mil. at each station. They are the main source of heat leak in the dipole and account for 4 w/magnet. The decentering forces due to the magnet field amount to 1.1 lb./0.001 in. (displacement) for each linear inch of coil. Decentering results mainly in quadrupole errors in the field - the higher multipole contributions being negligible due to the large distance between the iron and the active field region.

The yoke at present is 12 in x 15 in with a 7-1/2 in bore. It is stacked on a curved stacking fixture and the two halves forced around the cryostat and coil assembly. This results in a curved magnet, thus eliminating the sagitta of 0.5cm that would exist in a straight magnet. A considerable amount of waste results from stamping these laminations and a "no waste" shape has been devised and is being measured. A small amount of the iron in the lamination reaches the saturation level, however, the iron seems far enough away from the bore so that no undesirable

effects seem to propagate into the beam region. Almost \$300,000 can be saved if this lamination can be used.

Testing Program

The testing program has been divided into several independent efforts - vertical testing of the magnet coil, sans yoke, and cryostat, a complete analysis at the Magnet Test Facility, and systems tests to develop the pertinent information for design of the cooling system and the power supply and associated protection system.

Vertical Dewar Tests

In a vertical dewar test the coil is placed in a vertical dewar with boiling H₂ at atmospheric pressure. Quenches, when they occur, are detected and the power supply disconnected and the energy discharged into an external resistor. This generates an exponential discharge and a voltage of 2,000 volts across the coil terminals. The coil is instrumented to measure the change in diameter of the support collars during excitation and to record the motion of the wire of the inner coil next to the key. The number of quenches to train the magnet to its short sample limit, and the quench current vs. ramp rate are measured. These results are shown in the following figures.

Figure 2 shows a typical training curve. The wire for each magnet is tested and its short sample characteristics measured (shown in the insert). At this point, the high field point occurs at the inside end of turn of the inner coil. (Later, when the coil is in a yoke, the high field point is at the inner key.) A histogram of 20 coils tested is shown in Figures 3 and 4.

Figure 5 shows the deflection of the collars. The change in diameter is measured by means of calipers read out by strain gauges. The insert shows this change for a typical magnet vs. current which is very accurately parabolic as it should be. The histogram shows the behavior of a number of coils. A similar mechanical measurement measures the motion of the wire of the inner coil with respect to the key in the collar to verify directly that the coil has not lost its preload.

Additional measurements in this test are being superseded by those now being made at the Magnet Test Facility, which will be discussed below. See paper CA-15, 16.

Magnet Test Facility

At the outset it was realized that the ultimate verification of a properly constructed magnet can only be obtained by cooling it down and exciting it to full field. Consequently a Test Facility was constructed with six measuring stations using a 1,500W refrigerator. A magnet can be installed in a measuring station in four hours and cooled down in another four. Measurement at present takes about eight hours but this still represents a research program and is more complete than will be ultimately necessary. At present after cooling down and verifying the integrity of the vacuum system the following measurements are made:

1. Ramp rate dependence of the quench point.
2. Magnetization loss in magnet as a function of peak field.
3. Ramp rate dependence of loss.

4. Harmonic Analysis.
5. f B-dl vs. current.
6. B vs. z using NMR probe at 2T.
7. Orientation of field relative to the yoke and marking with survey flags.

The ramp rate dependence has given us a considerable amount of trouble. Early in the program, one foot test magnets were built which showed essentially no ramp rate dependence at ramp rates as high as 1T/s. More recently, the full size magnets have shown serious degradation at ramp rates as low as 0.2T/s. Fig. 6 shows the variation between good and poor magnets. The source of this change has been traced to eddy current losses in the coil cable.

The cable is made up of 23 strands of 0.027 in. diameter wire which has been coated with Stay-Bright. The inter strand resistance is low. Our early coils did not have sufficient pressure applied to them during the collaring process to ensure that when the magnet was cold there would be a preload on the coil greater than the magnet forces. In such a "floppy" coil the contact between strands would be poor, and hence eddy current losses in the cable would be low. The problem of preload was attacked and solved as described previously. However, the strands of the cable are now in excellent contact with each other and the eddy current losses become unacceptable. The losses cause heating in the magnet that increases with B and gave a bad ramp rate dependence to the coil. The obvious solution was to increase the inter-strand resistance while still keeping some contact between the conductors in order to help ensure current sharing among the strands. To this end we have tried several experiments, and several solutions have been found. The best seems to be giving the wire a treatment with Ebonol-C productive CuO layer. Table I lists the various magnets constructed and the loss in joules per cycle for a peak field of 4T and a ramp rate of .2T/sec. "Bismuth" means we tried to "poison" the Stay-Bright by dissolving 5% Bi in it. "Zebra" means cable made with 1/2 of the strands coated with Ebonol. This effectively breaks up strand-to-strand conduction, but leaves the top and bottom layers of the cable crossing in conducting loops. "Kapton" means that the Rutherford cable was formed over a 0.001 in. thick piece of Kapton 0.250 in. wide. (The Kapton survives the turks heads!). This essentially insulated one side of the cable from the other but left strand-to-strand contact through the Stay-Bright. Since the outer winding is in a much reduced field, we built two "graded" magnets with inner Ebonol coils and outers in the regular Stay-Bright configuration. The losses for a typical Stay-Bright coil made the same as the test series is shown for comparison.

Some typical measurements of the loss vs. peak field and at a fixed peak field vs. B' are shown in Fig. 7. For a triangular excitation, the losses should approximately follow the expression:

$$\text{Joules/cycle} = \alpha B_{\text{max}} + \frac{B B_{\text{max}}}{R}$$

The first term is the hysteresis losses, the second is the eddy current losses. Fig. 7 also shows the dramatic effect of the Ebonol insulation effectively reducing the eddy current losses to zero. RDD14 a normal Stay-Bright magnet is shown for comparison.

Harmonic Analysis

About 40 magnets have had a harmonic analysis made of their field. Roughly 20 of these only had their central field measured with a 4 foot long coil. The other 20 have each had a set of 3 overlapping measurements made with a coil 8 feet long - one in the center and one at each end. These three measurements can be combined to give an average through the magnet.

A brief word concerning the theory of the design of the magnet is in order here. First of all, if there are no construction errors, then by symmetry all of the skew multipoles are missing as well as the series of normal terms, quadrupole, octupole, etc. So we can expect the size of these terms to give some indication of the errors inherent in the magnet. Next there are two angles associated with the inner and outer coil, and hence the normal sextupole and decapole can be adjusted to zero in the body of the magnet. However, the ends must now be considered and here one finds a very strong sextupole moment plus some decapole. Hence, the angles are adjusted to eliminate the sextupole and decapole in the integral of B through the magnet. The resulting field is fairly rich in higher multipoles. Table II below shows the calculated multipoles in the body of the magnet as well as the average through the magnet including the ends. The units are in $10^{-4}T$ at 2.54cm when the central field is 4.5T.

We can now address the question of how well the present output from the "Magnet Factory" is matching the theoretically desired magnet. To clarify the nomenclature, we write here the field expansion used.

$$B_y(x) = B_0 \sum_{n=0}^{\infty} b_n x^n$$

$$B_x(x) = B_0 \sum_{n=1}^{\infty} a_n x^n \quad \begin{array}{l} \text{multipole number} = \\ 2(n+1) \end{array}$$

The terms in the expansion are measured up to the 30-pole term ($n = 14$). It is well to remember that a given multipole can be represented everywhere on a circle of radius r by a vector of fixed length but variable direction. The vector rotates n -times in proceeding around the circle and its length is proportional to r^n .

Two additional points are worth making. First, the field expansion is rich in harmonics. The higher harmonics essentially result from the sharp corners of the coil. We have very little control over these harmonics - errors in the winding would have to be pathological to strongly influence the $n = 14$ term. Hence, for these harmonics we can rely on theoretical calculations to tell us how important they are at any given radius provided we are not too near the coil. In our case, we find that at a radius of 1 in. the $n = 14$ term has $b_{14} \approx 10^{-5}$ or at a central field of 4.5T B_0 , $b_{14} \approx .4$ gauss. The higher terms are even smaller. Thus, everywhere inside of a 1 in. circle we will know the field to a relative accuracy of 1 part in 10^5 if we measure out to $n = 14$.

The second point is very important, and that is that the key angles effect mainly the low order harmonics, i.e., quadrupole, sextupole, octupole, decapole. Since these are easily adjustable, we see that we have a means of correcting systematic errors in the coils as they are manufactured. Thus, if the coils are made in a reproducible fashion by the "factory" we now are able to feed back measurement information to correct these low order multipoles.

Another way to summarize this is to say that any shape "near by" the desired shape of coil will have the same high harmonics as the "perfect" coil, but a different set of lower harmonics. However, these lower harmonics can be corrected in our coil by easily adjusted shims at the keys to produce the desired terms. It is in this fashion that we avoid having to produce coils with an absolute accuracy of the order of 0.001 in.

Now to examine the coils. Figures 8 and 9 show the average a_n and b_n of a set of 13 magnets in the series from 100 to 120. The horizontal axis is n and the vertical axis is $B_0 a_n$ and $B_0 b_n$ for $B_0 = 4.5T$. The error bars show the rms fluctuation about the average values. If there were no errors in the magnets, all of the a_n would be equal to zero as well as the odd b_n . It is seen that the major fluctuations occur in the quadrupole, sextupole, and octupole terms. This supports the thesis set forth above that these terms are mainly determined by the gross geometry of the coil. The even b 's should not be zero and the values calculated for them are shown in Table II.

It is seen in this set of magnets that the skew and normal quadrupole are both fluctuating about the same amount. (Table III gives numerical values.) The error driving a_1 is probably the asymmetry in the size of the top coil vs. the bottom coil. Each 0.001" that the "parting plane" deviates from perfect symmetry gives approximately 5 gauss at 1 in. for $B_0 a_1$. Similarly a right left asymmetry of the key angles of the inner coil of 0.002 in., we find, gives $B_0 b_1$ approximately 5 gauss at 1 in. Also the quadrupole is driven by displacement of the whole coil bundle from the center of the inner yoke. Calculation gives 1 gauss for the magnitude for each 0.001 in. displacement (in the obvious direction.) At present we think these errors are not out of line with our present construction errors.

The sextupole term b_2 is seen to be much too negative. This has been traced to the ends exhibiting a much stronger sextupole than calculations would indicate. At present, the details of this discrepancy are not understood. However, this effect can be corrected in the manner described above by compacting the inner and outer coils slightly more by means of shims at the keys. In this case we calculated an inner coil shim of 0.007 in. and one for the outer of 0.016 in. This change was made and the average coefficients of magnet #130 and 131 indicate that this change has corrected the trouble.

In addition to the harmonic analysis, the $B_y(z)$ is measured at 2T with an NMR PROBE. Short term fluctuation of the order of $\pm .05\%$ are evident and reflect errors in the conductor placement. The average value for 14 magnets is $9.984 \pm .004$ gauss/amp. The error if attributed completely to random fluctuations would indicate that the radius is fluctuating by $\pm 1.3 \times 10^{-3}$ inches.

The $\int B \cdot dl$ at various currents is also measured by stretching a single wire loop through the bore of the magnet and integrating the coil output as the magnet is ramped. The coil is flipped at zero current

to measure the residual field due to persistent currents. The $\frac{1}{l} \int B \cdot dl$ shows systematic effects due to persistent currents and very small non-linearities from the iron. This will have to be studied in more detail in order to ensure that the quads and dipole track. The average of $\int B \cdot dl$ for 10 magnets between units 110 and 130 is $9.985 \pm .005$.

Measurements are being undertaken to determine how stable the field is to temperature cycling and quenching. Due to the large amount of stored energy in a magnet, it is difficult to run meaningful life tests. However, mechanical cycling tests at low temperature are possible and are being carried out.

Quadrupole

The first quadrupole was a three shell quadrupole with the windings being wound somewhat after the BIL style. Eight such quads were built and tested. The experience with them was somewhat similar to that with dipoles. With the completion of the eight three-shell quads we have switched production to a two-shell quad with a spacer in the inner coil to help control the harmonic content of the field. The first model of this coil has just been tested and after two quenches we were unable to follow its training beyond the 5400 amps limit set by the power supply. The coil package is well clamped and shows no evidence of motion under magnetic forces. Complete measurements are underway.

The quad-package also houses the beam position detector, the tune quadrupole, the vertical and horizontal dipole and sextupole correction coils. The safety lead for magnet protection and liquid helium and nitrogen connections are made, when necessary, in a box.

Present Program

The present program has the following major goals.

1. Increasing dipole production from 5 to 8 magnets/week, while controlling the quality. Every magnet will be tested and pass acceptance criteria.
2. Complete the new quadrupole assembly line.
3. More tests on strings of magnets under Laboratory conditions to verify that the magnet power supply and quench protection scheme is satisfactory. (Paper JC-8)
4. A major effort is underway to install a full sector of the machine. It will allow us to investigate injection into a string of 160 dipoles and study the cryogenic problems of the first large installation of superconducting magnets. Twenty magnets are now installed and cold and early '79 should see the sector complete. An ingenious scheme conceived by T. Collins will possibly enable us to achieve the circulating beam through this sector. The experience in the tunnel has been as follows. Two men for one hour can transport and set a magnet in place. One man two hours to connect vac/He/electrical connections. Two men two hours to align. Leaks have occurred once about every 4 magnets. It is expected this will decrease as the crews become more experienced with cryogenic magnets.
5. Finish the central helium liquifier and bring it on-line.

Future Challenge

On the basis of our experience so far we can identify the new challenging problems that a 5 TeV or greater energy machine poses.

1. Develop an 8.0T (or more) magnet.
2. Perfect schemes to make an inexpensive "extruded" magnet of high quality. Since only the cross section is important, the tooling should reflect this and become independent of length.
3. Develop the technology of handling beams in a small aperture. It is well known that the aperture in the past has been determined by the need to inject, extract, stack, etc. However, with large fields, the forces become very large and the energy density high. In addition, with superconducting magnets, the energy necessary to quench may only be fractions of milli-

joules/cm³, while the beam may store 10 M joules or more. The tendency is to want a large aperture to keep the beam halo away from the magnet! However, a small aperture is strongly indicated by magnet cost, by large constraining forces, and by the large energy density in an 8T magnet.

It will be a real challenge to reconcile these conflicting requirements and invent solutions using the new magnet technology.

This is a report on the combined work of many people at Fermilab. Some of this is indicated by references to other papers given at this conference. However, I would like to acknowledge that the guiding hand of R.R. Wilson prevades all of the work and the sculptural beauty of the magnets attests to his presence.

TABLE I.

Joules/Cycle ($B_m = 4T, \dot{B} = .2T/sec$)

	1	2	3	4	5
Hysteresis	400	400	300	390	410
Eddy Current	0	30	0	100	720

1. Ebonol
2. Eboncl Inner Coil
Stay-Bright Outer
3. Zebra + Kapton
4. Zebra
5. Stay-Bright

TABLE II

Normal Multipole Moments* as Designed and Measured

	b_2	b_4	b_6	b_8	b_{10}	b_{12}	b_{14}
Body	24	12	21	-55	17	-4	.3
Integral	.2	4	20	-54	16	-4	.3
Measured	-60 ± 38	10 ± 5	16 ± 2	-59 ± 2	20 ± 1	-5 ± 1	$.1 \pm .5$

*Units gauss at 1: when $B_0 = 4.5T$.

TABLE IIIa

Skew Multipole Moments as Measured (13 Magnets)

	a_1	a_2	a_3	a_4	a_5	a_6	a_7	a_8	a_9	a_{10}	a_{11}	a_{12}	a_{13}	a_{14}
av	7	2	.3	-.1	0	0	-.4	-.2	.1	-.5	.3	.7	.3	-.1
rms Δv	13	2	4	.7	1.5	1	2	3	.2	1	.6	.9	.8	.6

TABLE IIIb

Odd Normal Multipole Moments as Measured (13 Magnets)

	b_1	b_3	b_5	b_7	b_9	b_{11}	b_{13}
av	11	3	.7	1	-.1	-.1	.1
rms Δv	16	2	1	2	.2	.6	.7

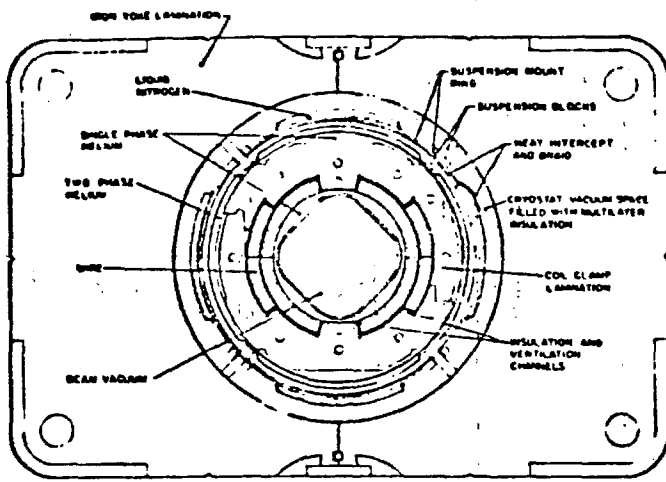


Figure 1. Dipole Magnet Cross Section.

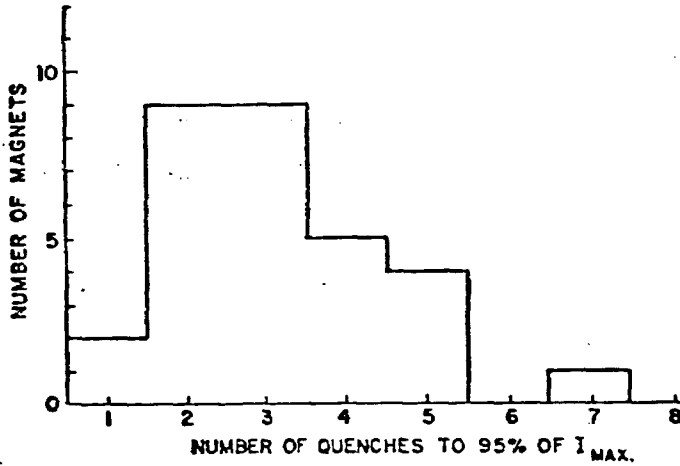


Figure 3. Training Current Distribution.

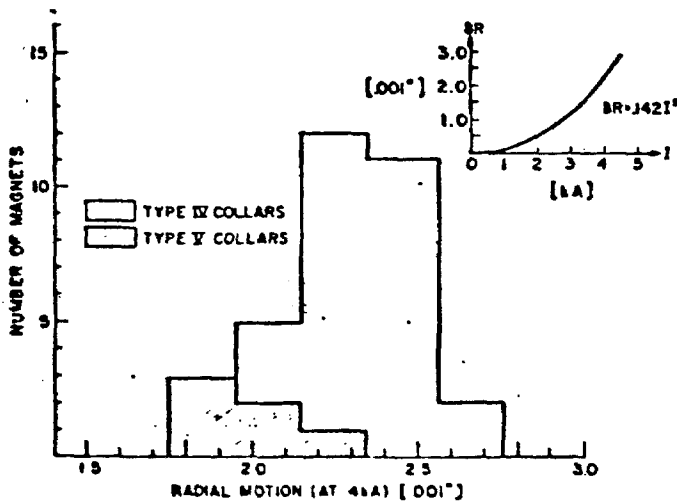


Figure 5. Elastic Radial Deformation

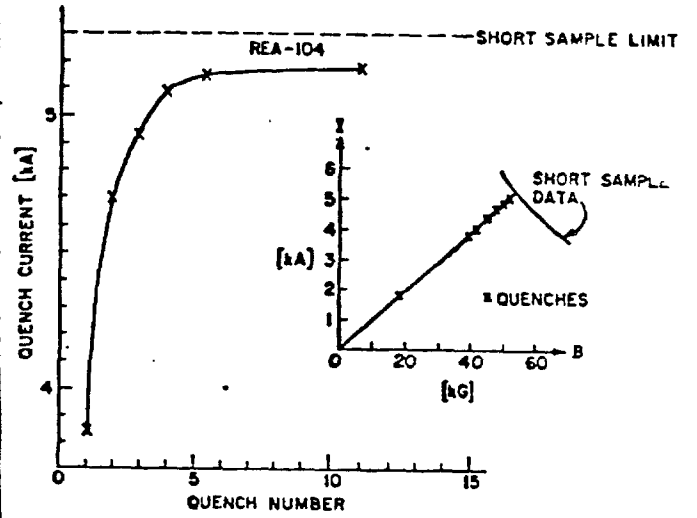


Figure 2. Training Curve.

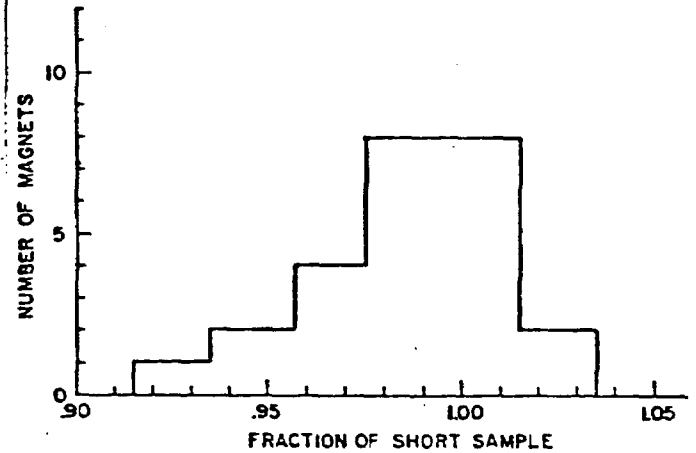


Figure 4. Distribution of Final Training Current as a Fraction of Short Sample Limit.

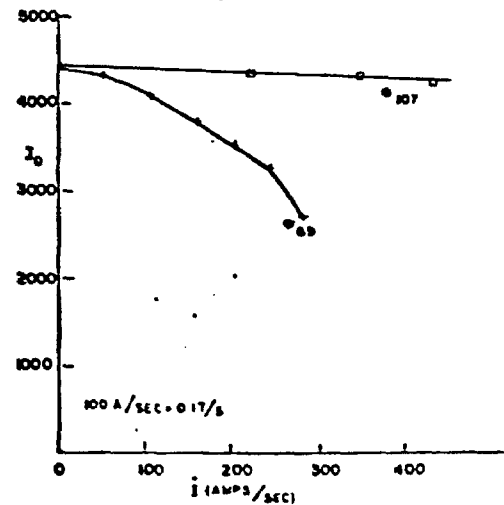


Figure 6. Quench Current vs. Ramp Rate

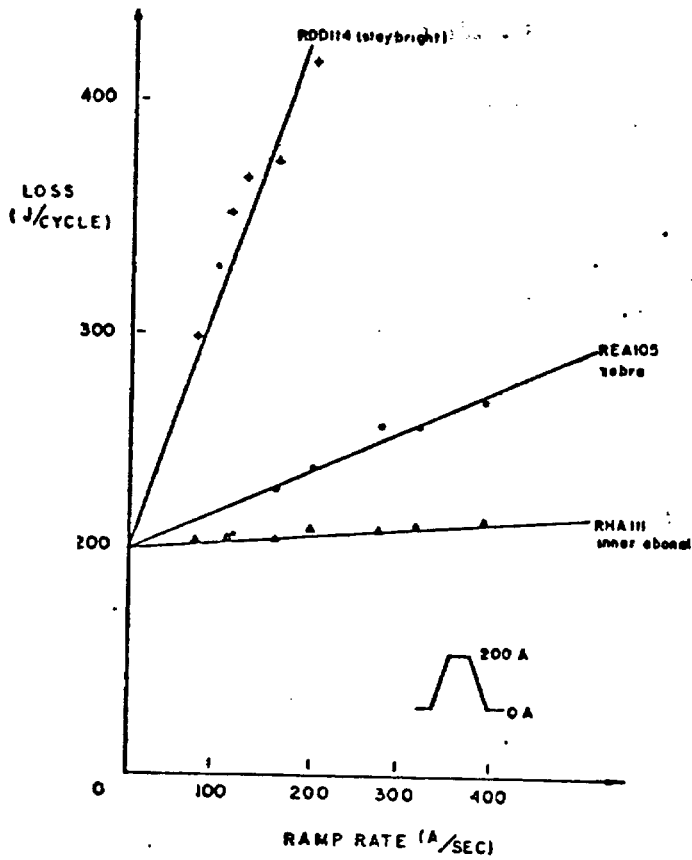


Figure 7. Energy Loss vs. Ramp Rate.

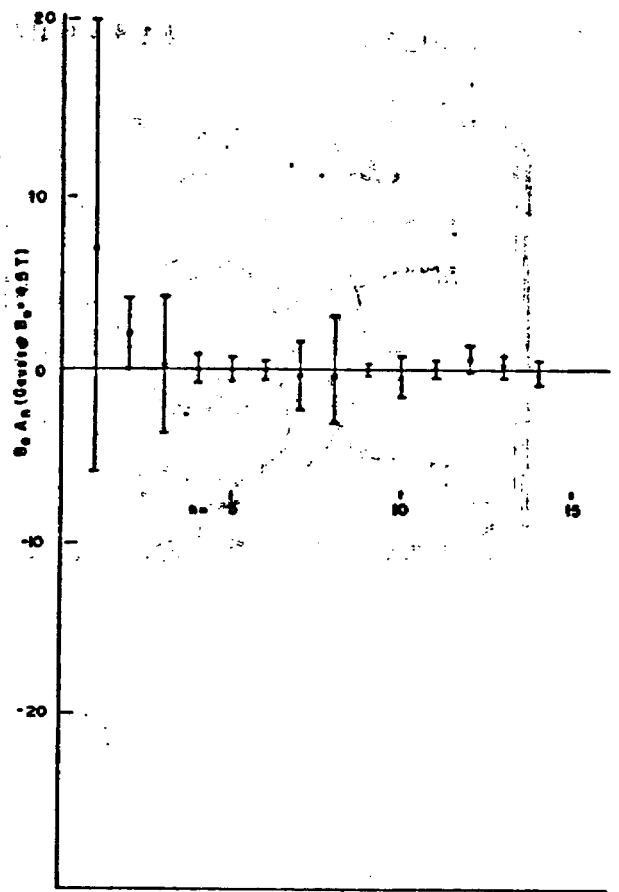


Figure 8. Skew Components at 3T Bore Field.

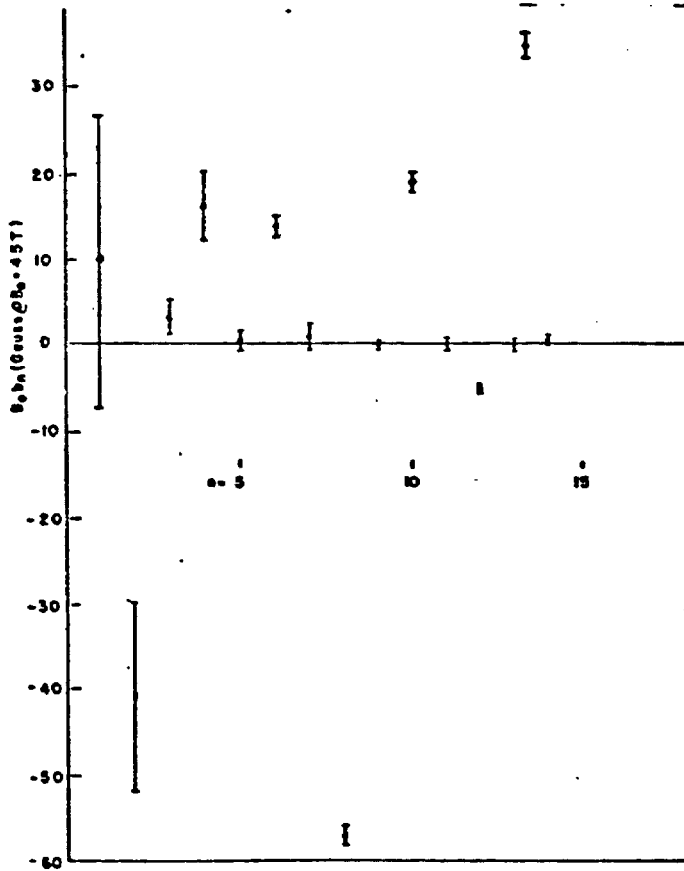


Figure 9. Normal Components at 3T Bore Field.